2026 ASEE ANNUAL CONFERENCE June 21–24, 2026 | Charlotte Convention Center, NC
Host Sponsor UNC Charlotte
Paper ID #53344

Redesigning a Canonical Fluid Mechanics Experiment: Coupling Computational and Experimental Approaches

Dr. Arturo Cajal, California Polytechnic State University, San Luis Obispo

Arturo Cajal holds a Ph.D. in Mechanical Engineering with expertise in aerodynamics and computational fluid dynamics (CFD). His work integrates computational and experimental methods to improve engineering education. Arturo is passionate about introducing CFD to undergraduate students to strengthen their technical foundation and curiosity in fluid mechanics, helping them develop both analytical and practical skills essential for solving modern engineering challenges.

Dr. Hans C. Mayer, California Polytechnic State University, San Luis Obispo

Dr. Hans Mayer holds a BSME degree from Cal Poly SLO, an MS degree in ME from Carnegie Mellon University, and a PhD in ME from the University of California Santa Barbara. He has approximately 16 years of teaching experience as both a lecturer, tenure-track, and tenured faculty member in the Mechanical Engineering Department at Cal Poly SLO, and enjoys finding new ways to get students interested in fluid mechanics through hands-on teaching labs and other student-centered research projects.

Redesigning a Canonical Fluid Mechanics Experiment: Coupling Computational and Experimental Approaches

<u>Abstract</u>

As computational tools become more accessible, the need to train engineers with strong software skills has become increasingly prominent. Within the field of fluid mechanics, Computational Fluid Dynamics (CFD) stands at the forefront of modern computational methods. The work presented in this paper aims to redesign a traditional undergraduate fluid mechanics laboratory experiment so that it integrates CFD with classical experimental approaches. In other words, unlike a traditional CFD exercise that has no experimental component, and in contrast to a traditional undergraduate fluid mechanics laboratory experiment that might have no computational counterpart, we envision a seamless blend of these two activities so as to have students recognize that an experiment, when properly designed and implemented, can serve the purpose of a CFD *validation* while still meeting the traditional learning objectives of each separate entity.

The uniform flow past a circular cylinder is selected as the canonical configuration to validate CFD results. This configuration is selected because it provides valuable insights into how different flow conditions influence the forces acting on bodies submerged in fluids. Additionally, the lack of complexity of the model geometry makes it well-suited for a variety of undergraduate labs that may or may not have extensive experimental equipment, i.e., complex aerodynamic models or measurement instruments. The testing campaign for this work will be performed using an Engineering Laboratory Desing wind tunnel model 406, and the simulations will be carried out using OpenFOAM, an open-source partial differential equations solver that is widely used in industry and academia. We begin with an overview of the introduction to CFD that can be completed by a student outside of the laboratory. This element of the lab is designed to help students understand the complete workflow of a CFD simulation, starting from problem definition and preprocessing to data collection, postprocessing, and effective reporting of the computational results. Along the way, students are tasked with providing choices for the CFD simulation through directed prompts. These choices leverage and reinforce their current understanding of the flow all the while providing insight into the CFD simulation process (e.g., A question like - Well upstream of the cylinder, what characteristics can we anticipate the flow field to have? – serves to introduce the need for velocity and pressure boundary conditions.). Once completed, important quantities from the simulations including surface pressure distribution, viscous drag, separation point estimation, and near and far field flow visualization can be extracted. With these key computational results in hand, students are then directed to think of the hands-on laboratory experiment that follows as a CFD validation study wherein all of the important results just mentioned can be measured or recorded from the experiment (e.g., surface pressure distributions from static pressure tap(s), wake velocity profiles obtained with a Pitot-static tube traversed through the flow, and creative qualitative flow visualization using photographs of tufts). While performing this experiment, students gain hands-on experience with these tools and measurement techniques. This redesigned experiment helps students establish both quantitative and qualitative expectations using CFD before performing the physical study. Examples include using ranges of static pressure from the CFD simulations to consider whether the instruments available to them – like a pressure

transducer – are appropriate for the experiment, or estimating the size of the wake from the CFD study to set the bounds for the wake traverse measurements. Overall, this integrated approach aims to strengthen theoretical knowledge, improve intuition, and enhance students' technical and experimental skill sets by rethinking how a traditional undergraduate fluid mechanics experiment can be paired with the introduction of CFD simulations.

Introduction

One of the biggest challenges in physics is finding exact solutions to the Navier-Stokes equations (NSE), which govern the motion of Newtonian fluid flow. Common examples of such fluids include air, water, and oil, as encountered in the majority of modern engineering systems. Traditional fluid mechanics analysis methods are categorized into three principal approaches: analytical solutions, experimental investigation, and computational modeling, as presented in Figure 1.

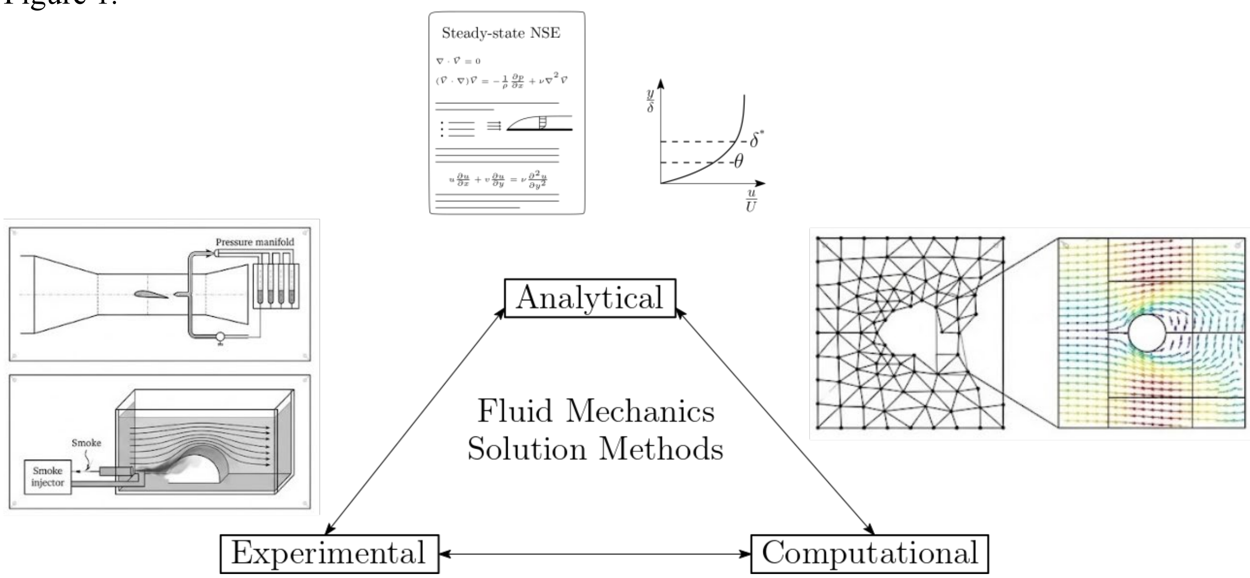

Figure 1. Three main approaches to resolve contemporary fluid mechanics problems. While all are relevant and leverage the appropriate strengths of each other in modern engineering problems, students are often – in traditional learning environments - only exposed to the approaches independently or, at most, in pairs.

Analytical solutions typically rely on significant assumptions that reduce the complexity of the governing equations to canonical configurations. While these solutions provide insight into flow physics and remain indispensable for building a foundational understanding, they often lack the geometric and physical complexity characteristic of contemporary engineering systems. Consequently, their range of direct applicability is limited. Experimental analysis offers direct physical evidence of flow behavior through pointwise measurements and flow visualization techniques. These methods play a critical role in developing physical intuition, uncovering previously unrecognized flow features, and validating theoretical models. However, experimental investigations are frequently constrained by facility space and instrumentation availability, particularly in undergraduate laboratory environments. Computational methods, specifically Computational Fluid Dynamics (CFD), offer a means to partially alleviate these constraints by providing approximate numerical solutions at discrete locations for two-dimensional and three-

dimensional flow configurations. Furthermore, advances in computational power and the widespread availability of open-source solvers have made CFD an essential tool in modern engineering practice.
Classic undergraduate fluid mechanics curricula, developed to a large extent prior to the advent of modern computing resources, typically integrate the analytical and experimental pillars by comparing textbook solutions with selected laboratory experiments to reinforce fundamental concepts (and this is in an advantageous situation where a laboratory is available). While this traditional approach effectively supports conceptual understanding, the computational component is often omitted, treated as a separate exercise, or isolated and covered in an entirely separate advanced course. When included, CFD activities are frequently limited to comparisons with analytical solutions, with little emphasis on experimental validation. As a result, students are rarely exposed to the integrated analytical-experimental-computational workflows that characterize contemporary engineering practice.

The present work seeks to address this gap by constructing a deliberate bridge through a blended laboratory methodology. Rather than positioning CFD as a post-hoc verification tool or as an isolated numerical exercise, simulations are introduced as a predictive framework that informs experimental design, measurement strategy, and data interpretation. By transitioning from a traditional stand-alone laboratory experiment to a CFD-driven validation, students are required to justify experimental decisions, assess discrepancies between numerical predictions and laboratory measurements, and articulate potential sources of error. In this way, the laboratory experience is shifted toward an inquiry-based format, encouraging students to move beyond procedural execution and data collection and toward reflective data acquisition decision-making.

Prior work has largely relegated CFD to a supporting role characterized by limited portability and capability. Some approaches have proposed in-house alternatives [1, 2]; however, while these help introduce the CFD workflow, they often lack robustness. Such packages require learning niche workflows and are rarely portable, as software and hardware updates often lead to highly specific debugging issues. Consequently, CFD is frequently used only as a "pre-lab" visualization [3, 4] or a post-hoc comparison to analytical theory [5-7].

The objective of this study is to move beyond these isolated exercises toward an integrated approach where students must design an experimental campaign based on numerical predictions. By requiring students to validate CFD results against their own gathered experimental data, the curriculum shifts from procedural data collection to a standardized method of engineering validation. This ensures that CFD is utilized as a functional design instrument rather than merely a visualization aid.

This integration is particularly relevant for maintaining alignment with ABET accreditation criteria [8], which emphasize the development of engineering judgment and the ability to interpret data in the presence of uncertainty as highlighted by their areas of quality assurance. Additionally, the authors envision that such an approach will be appealing to students who want to incorporate more computational methods in their undergraduate curriculum all the while maintaining hands-on experiential learning opportunities with hardware-based experiments.

Blended Experimental-Computational Methodology

A wind tunnel is a primary instrument used in fluid mechanics to characterize the aerodynamic performance of bodies moving submerged in fluids. In traditional undergraduate laboratory wind tunnel experiments, the workflow typically follows a series of predefined steps. Students often perform data collection based on established instructions with little opportunity to make informed decisions regarding equipment selection or key data acquisition locations. In this traditional model, the comparison to analytical or numerical data occurs only after the experiment is completed; therefore, the student role is primarily procedural rather than investigative. This means that while students gain hands-on experience with hardware, they are often unaware of the details associated with why they are collecting certain data and in such a way as outlined in the procedures of lab manuals.

In contrast, CFD methods provide approximate solutions that can inform the experimental process before it begins. These simulations assist in making decisions regarding the instrumentation available in a laboratory facility. For example, if the pressure distribution around a body is simulated beforehand, the resulting pressure magnitudes guide the selection of a manometer or transducer with an appropriate range. Similarly, predicting regions of steep physical gradients allows students to optimize data acquisition. If a separated boundary layer is expected, the predicted shear stress distribution indicates the location of the separation point; this suggests a higher density of measurements in that specific region to better characterize the phenomenon.

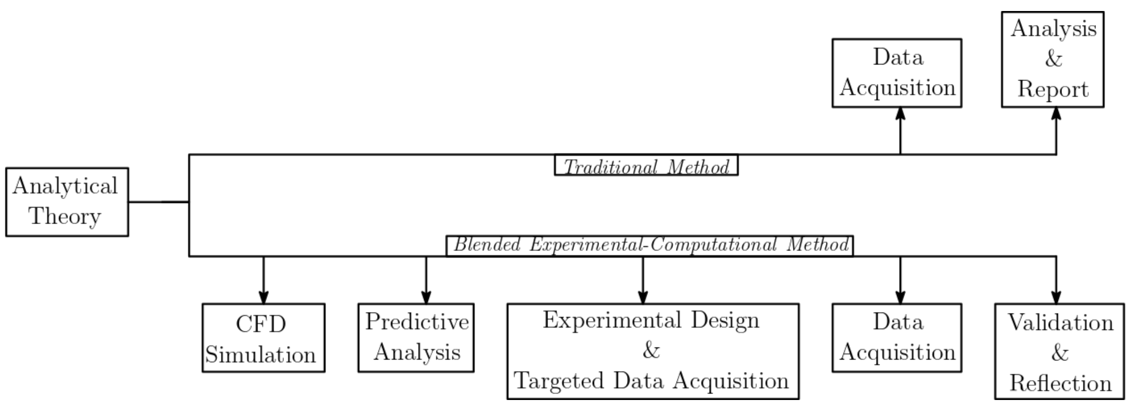

Figure 2. A traditional versus blended experimental-computational approach to undergraduate experiment workflows. The upper branch represents a traditional method where student involvement is more procedural. The lower branch that is explored in this paper allows the student to be more investigative and have greater agency in both the design and implementation of the experiment.

The proposed *Blended Experimental-Computational Methodology* differs by requiring a *CFD Simulation* immediately following the *Analytical Theory* phase, enabling thus, an *Experiment Design and Targeted Data Acquisition* stage, before Data Collection. This novel step includes a pre-laboratory assignment where students are guided through a prompt-based task to compute the initial and boundary conditions necessary to run the model. To ensure the pedagogical focus remains on fluid physics rather than software troubleshooting, a template is provided so that students only modify quantities relevant to the specific case.

Instructors should carefully design this step to limit the simulation scope. Student tasks include computing free-stream flow quantities from given Reynold, *Re,* and Mach, *Ma*, numbers or defining the boundary conditions for a given configuration, i.e., no-slip, no-penetration condition for a viscous wall. Regarding simulation controls—such as time-step size, iteration count, numerical schemes, and solution algorithms—it is strongly encouraged that the instructor limits student interaction with these parameters, as these involve advanced numerical analysis typically reserved for graduate studies. Keep in mind that the purpose here is to introduce the utility and high-level basics of CFD simulations encountered in modern engineering problem solving without being the sole focus of the laboratory exercise. Instead, students should see it as a complementary tool, with encouragement to explore further in advanced classes if the student so chooses.

Following the *CFD Simulation*, the methodology transitions to a *Predictive Analysis* stage. In this phase, students use CFD results to forecast flow quantity ranges and identify specific regions of interest, such as pressure and shear stress distribution or boundary layer and wake features for wall-bounded viscous flows. This allows students to predict the expected flow characteristics before entering the laboratory.

Based on this analysis, the next stage in the blended methodology is the *Experimental Design and Targeted Data Acquisition.* For the former, the necessary equipment to perform the experiment is selected. Rather than following a rigid set of instructions, students select the optimal instruments from a predefined inventory (this inventory would be site specific). For instance, if surface pressure is required, students may choose between a digital pressure transducer for discrete readings or an analog transducer connected to an oscilloscope to capture time-varying data. This forces students to justify their instrumentation based on the predicted flow behavior observed in their CFD models. Similar to the CFD template, the instructor is strongly encouraged to limit this list to include items that are relevant for the scope of the experiment. For the *Targeted Data Acquisition*, students leverage computational insights to execute the physical experiment. More specifically, regions of interest are selected where stiff numerical gradients affecting the aerodynamic performance of the body exist.

The framework concludes with *Validation and Reflective Decision Making*. Students must analyze why experimental results deviate from CFD predictions, performing a critical assessment of numerical assumptions, such as turbulence models, and physical limitations, such as wall interference or freestream turbulence. By closing the loop between prediction and measurement, students gain a deeper understanding of the interplay between theory, computation, and physical reality. This deeper understanding is essential for the more challenging problems that they will encounter in industry or academia.

Example of Implementation of the Blended Experimental-Computational Methodology

This section demonstrates the implementation of the *Blended Experimental-Computational Methodology* at California Polytechnic State University, San Luis Obispo (i.e., Cal Poly). The selected test case is the uniform flow past a cylinder simulated using the Finite Volume Method (FVM), and results are validated using an incompressible wind tunnel. The reason for choosing this as a test case is that it leverages a pre-existing traditional method experiment that has already been in practice at Cal Poly for nearly 20 years. Furthermore, since the traditional experiment is based on equipment that is available commercially from suppliers of academic wind tunnels, it is anticipated to be directly applicable to a great number of colleges and universities.

Example of Implementing Analytical Theory Stage

The first stage of the framework is the *Analytical Theory*, where a canonical fluid mechanics problem is analyzed using first principles. The selected configuration for this study is the uniform flow past a cylinder.

Uniform Flow Past a Cylinder

Uniform flow past a cylinder is a cornerstone configuration in engineering. Despite the simplicity in shape, it exhibits a rich set of flow field behavior (i.e., variations in velocity and pressure) depending on the magnitude of the Reynolds number, Re_D, which expresses the ratio of inertial to viscous forces and is defined as

$$Re_{\mathrm{D}} = \frac{\rho U D}{\mu}, \tag{1}$$

where ρ, U, and μ are the fluid's density, velocity, and viscosity, respectively; and the diameter, D, is the characteristic length. This complex behavior can be captured in the resulting drag force, F_D, and dimensionless drag coefficient, $C_D = F_D/(1/2)\rho U^2$, which is shown in Figure 3.

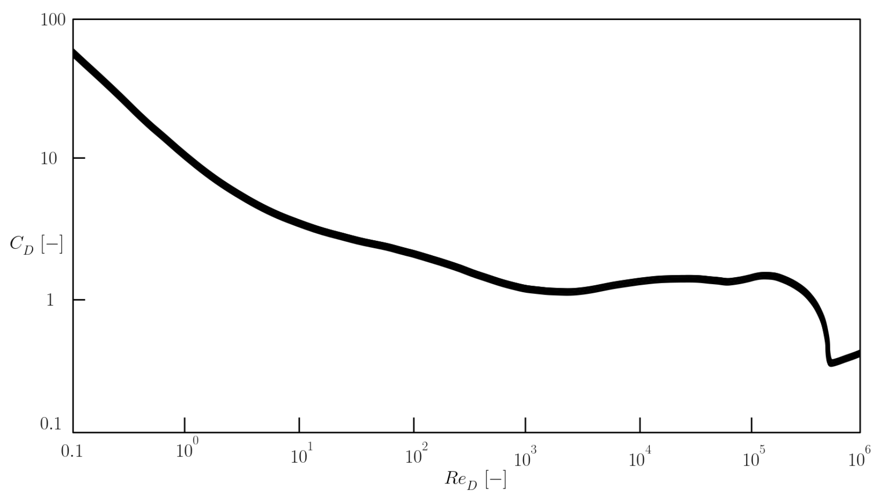

Figure 3. Coefficient of drag versus Re_D for a cylinder in uniform flow. The drag coefficient is nothing more than a normalized drag force. Adapted from [9].

Why does C_D capture this complexity of flow field behaviors? Because drag is nothing more than the streamwise component of the total surface force acting on the cylinder surface area A (equation 2) – and as such it is comprised of a surface pressure component (form drag) and a surface shear stress component (skin friction).

$$F_D = \left[\int_A p d\vec{A} + \int_A \vec{\tau}_w dA\right]_{\text{in direction of } U} \tag{2}$$

Thus, solving for the resulting flow field past a cylinder in a uniform flow yield details of velocity $\vec{V}(x, y, z)$ and pressure $p(x, y, z)$ that can ultimately yield drag force or its dimensionless counterpart, and really yield any desired aerodynamic information about the cylinder. Hence the solution to the flow field serves, effectively, as the *Analytical Solution* in this exercise. Similar situations to this are: solving for the velocity profile for fully developed laminar flow in a pipe (which can yield shear stress and pressure loss information) or solving for the flow field associated with spin coating of a film (which can yield time-dependent film thickness behavior). However, unlike those last two examples what we can recognize or anticipate is that for the cylinder, with the exception of very low Reynolds numbers, i.e., $Re_D << 1$, the coupled velocity fields and pressure fields cannot truly be solved using analytical techniques over the entire range of Re_D and in particular the high values of Re_D accessible in most laboratory wind tunnel facilities because of the constraints associated with large characteristic lengths, the fluid properties of air, and the moderate velocities created by wind tunnel fans. For instance, Cal Poly utilizes a 2-by-2 foot wind tunnel capable of achieving a maximum Reynolds number of $Re_{\max} \approx 10^5$ for models spanning the whole test section, where wall blockage effects become relevant.

So, although we treat this as the *Analytical Solution* stage for this particular experiment, we can conclude that there is no typical analytical solution that can be compared to (in contrast to many undergraduate fluid mechanics problems). There are only the known and collective results of a variety of solution techniques that form summative information as presented in Figure 3, which students can treat as an analytical solution, or known solution (and not a CFD solution), for the purposes of this particular experiment.

For this work the case definition is given in Figure 4. The freestream values correspond to values that are characteristic of the wind tunnel used for this experiment in Cal Poly. In particular, the Reynolds number corresponds to a subcritical condition with a laminar boundary layer that will separate to form a wake. This is a value of Re_D below the sudden "drag crisis" dip in the curve shown earlier in Figure 3. For the CFD simulation it is not important that students select a Reynolds number. This could be a condition that is established for which they have no control (in contrast to choices made to design the experiment to allow for relevant measurements at this value of Re_D).

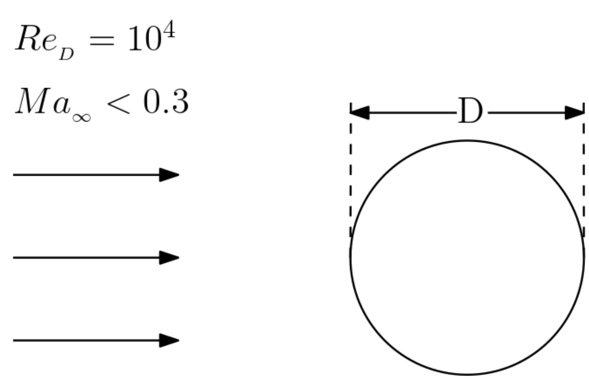

Figure 4. Selected flow configuration. The Reynolds number is selected since the experimental set up uses a similar value. A Mach number less than 0.3 ensures incompressible flow.

Example of Implementing CFD Simulation Stage

Following the *Analytical Theory* stage, students perform the *CFD Simulation*. In this phase, an introduction to CFD is given followed by the derivation of initial and boundary conditions to conclude with running the simulation.

Introduction to CFD

CFD is presented here as a numerical approximation of the partial differential equations (PDEs) governing viscous fluid flow at discrete points in space. While various discretization methods exist, the emphasis in this framework is placed on the FVM, as used in majority of research and commercial software.

As with the analytical solutions, the scope and complexity of the simulations are intentionally limited by the physical flow configurations. In this work, simulations are restricted to incompressible, steady-state flows. This approach yields a numerical approximation of the more complex, three-dimensional, and unsteady flow encountered in the actual wind tunnel.

These assumptions and simplifications are strategically chosen to limit the scope of the instruction to fundamental concepts. In this regard, the curriculum focuses on steady-state simulations using Reynolds-Averaged Navier-Stokes (RANS) models to account for turbulence within incompressible flows.

Finite Volume Method (FVM)

Students are introduced to FVM as a method where the flow domain is discretized in finite control volumes (CVs) and the governing equations, the incompressible Navier Stokes equations, are enforced and integrated at cell, subject to specified initial and boundary conditions.

The solver proceeds iteratively until a convergence criterion is achieved - typically defined by the relative change between solutions at successive iterations. Once the residuals fall below a predefined threshold, i.e. 10^{-6} as in the results presented in this work, the solution is considered converged, indicating that no significant changes in flow quantities or integral performance parameters, like drag or lift, remain.

Two important aspects of the use of FVM are turbulence modeling and grid independence studies. Next a brief description of the contents regarding this is presented.

Turbulence Modeling

To account for the turbulence characteristic of high Reynolds number flows, the Reynolds-Averaged Navier-Stokes (RANS) equations are utilized to model this effect. These equations introduce a new variable, the Reynolds Stress Tensor (RST), $-\overline{u_i' u_j'}$, representing turbulent fluctuations in the flow. Using the Boussinesq hypothesis, where turbulence is represented as an augmented viscosity, students explore the concept of Eddy Viscosity, ν_t:

$$-\overline{u_i'u_j'} \propto \nu_t \,. \tag{3}$$

The RST represents the momentum exchange due to turbulent fluctuations. It is important to emphasize that ν_t is a property of the flow, not the fluid, and is calculated using RANS models. For this example, the Shear Stress Transport (SST) turbulence model [10] is selected for this work, where $\nu_t = k/\omega$. But for deeper technical exploration, students are redirected to the NASA Turbulence Modeling Resource (TMR), hosting state-of-the-art RANS turbulence modeling, to understand the capabilities of different RANS models.

Grid Convergence

Although students are provided with a functional baseline mesh that balances computational cost and accuracy to perform this activity, a critical learning outcome in this stage is the Grid Convergence Study. Grid convergence ensures that the solution is grid-independent, meaning that further refinement of the mesh no longer significantly changes the results of the quantities of interest. To facilitate this, a family of nested grids is provided, allowing students to perform an optional independence study. By evaluating these varying mesh densities, students learn to balance the trade-off between computational overhead and numerical fidelity.

Derivation of Initial and Boundary Conditions

At this stage, students are guided through a targeted set of prompts to define initial and boundary conditions that directly correspond to the laboratory's physical configuration. This ensures that the numerical model is a faithful representation of the experimental environment.

Given the problem definition in Figure 4, students are required to calculate both initial and boundary conditions for mean flow and turbulence quantities. Table 1 summarizes the freestream initial values for the case analyzed in this work.

The mean flow quantities are derived from the target Reynolds number, assuming the fluid is air modeled as a calorically perfect gas at standard sea level conditions. Furthermore, a diameter, D = 1 [m], was used to construct the mesh. For the turbulent freestream conditions, a turbulence intensity, $I = u'/U$, of 0.15% and a viscosity ratio, $\nu_t/\nu = 0.1$, are defined, which are characteristic of low-speed wind tunnels. The intensity, I, accounts for the turbulent fluctuations in the freestream; while modern wind tunnels provide a highly uniform inlet flow, mechanical vibrations from the power system invariably introduce small-scale fluctuations. Furthermore, the viscosity ratio compares the turbulent eddy viscosity to the molecular viscosity. For configurations like the facility at Cal Poly, a low freestream viscosity ratio is a representative approximation, assuming that turbulent dissipation in the freestream is significantly lower than in the wake or boundary layer regions. Based on these values, the k - ω model provides the necessary framework to compute turbulent kinetic energy, k, and the specific dissipation rate, ω, at the freestream.

Table 1. Mean and turbulent flow free stream values. The fluid considered is air at standard sea level conditions with a kinematic viscosity, $\nu_{air} = 10^{-5}$ m^2/s, representative of laboratory conditions. The grid family has been constructed such that, D = 1 m. By fixing the viscosity and the characteristic length, the velocity is the only variable to left for adjusting the Reynolds number.

Flow variable	Equation	Free stream value
Velocity	$U = \frac{Re_D\ \nu}{D}$	0.1461 $[m/s]$
Pressure	p = 1 atm	101.325 [kPa]
Turbulent kinetic energy	$k = \frac{3}{2}(U\ I)^2$	$3.2 \times\ 10^{-6}[m^2/s^2]$
Turbulence specific dissipation	$\omega = \left(\frac{k}{\nu}\right)\left(\frac{\nu_t}{\nu}\right)^{-1}$	0.219 $[s^{-1}]$
Turbulent eddy viscosity	$\nu_t = \frac{\rho k}{\omega}$	$1.46 \times 10^{-5}\ \ [m^2/\ s]$

Running the Simulation

At this stage, students are directed to download an online repository containing a case directory for OpenFOAM. This software is selected because it is an open-source distribution widely used in both industry and academia, making it ideal for reproduction across various educational institutions. For this specific implementation, OpenFOAM version 8 is utilized. A fundamental incompressible, steady-state simulation in OpenFOAM requires three essential subdirectories: *0, constant, and system.*

- The *0* directory: Contains the initial and boundary conditions for all solved flow variables. Students must modify these files to reflect the values calculated in Table 1.
- The *constant* directory: Hosts the mesh, physical fluid properties, and turbulence model selections. Students input the relevant fluid constants here. No modifications are required to this folder, unless a grid convergence study is desired. For which the *polyMesh* directory would need to be modified accordingly.
- The *system* directory: Controls the numerical schemes, solution algorithms, and post-processing activities. This directory contains files that require no modifications from the students; however, they have been thoroughly commented to guide students through the numerical logic. Since the proper modification of these parameters typically requires graduate-level training, student interaction with these files is intentionally minimized to keep the focus on fluid physics.

Modifications to the 0 Folder

The *0* directory stores the initial and boundary conditions for the flow variables derived in Table 1. Figure 5 illustrates the modifications made to the velocity file, *U*. Specifically, the freestream value is modified to *(0.1461, 0, 0)*; this corresponds to a uniform flow in the *x*-direction with a magnitude of 0.1461 m/s. Also, the velocity vector at the cylinder surface is (0, 0, 0), imposing the no-slip and no-penetration boundary conditions.

```
/*--------------------------------*- C++ -*----------------------------------*\
  =========                 |
  \\      /  F ield         | OpenFOAM: The Open Source CFD Toolbox
   \\    /   O peration     | Website:  https://openfoam.org
    \\  /    A nd           | Version:  8
     \\/     M anipulation  |
\*---------------------------------------------------------------------------*/
FoamFile
{
    version     2.0;
    format      binary;
    class       volVectorField;
    location    "0";
    object      U;
}
// * * * * * * * * * * * * * * * * * * * * * * * * * * * * * * * * * * * * * //

dimensions      [0 1 -1 0 0 0 0];

internalField   uniform (0.1461 0 0);

boundaryField
{
    cylinder
    {
        type            fixedValue;
        value           uniform (0 0 0);          (a)
    }
    inlet
    {
        type            fixedValue;
        value           uniform (0.1461 0 0);     (b)
    }
    outlet
    {
        type            zeroGradient;             (c)
    }
    BaseAndTop
    {
        type            empty;                    (d)
    }
}


// ************************************************************************* //
```

Figure 5. Modified velocity field, *U*, file in the *0* directory. (a) At the cylinder a *fixedValue* of *(0, 0, 0)* is assigned, as for a viscous wall. In contrast, (b) at the inlet (free stream) a value of *(0.1461, 0, 0)* is assigned. (c) The outlet boundary is set to *zeroGradient*, as no flux returns to the flow domain. Finally, (d) the *BaseAndTop* boundary remains empty, as this is a two-dimensional simulation.

Similarly, for turbulent quantities, the turbulent kinetic energy, *k*, specific dissipation, *omega*, and turbulent viscosity, *nut*, files are modified to match the values computed in Table 1. To exemplify this process, Figure 6 shows the specific modifications made to the *k*-file.

Optional Modifications to the constant Directory

The *constant* directory contains two primary files and one subdirectory, *polyMesh*. The latter contains the mesh; students are only encouraged to modify this subdirectory if a grid convergence study is being performed. The first file is called *turbulenceProperties* defining the turbulence model to be used; in this framework, no modification is required for this file. Finally, the *transportProperties* file stores the molecular viscosity of the fluid. Because this value is given to the students no modifications are needed. However, if a viscosity swept is required to vary the Reynolds number, it could be modified in this file. Once the *0* folder is modified with the correct freestream values, the case directory is submitted for computation. Results are typically returned within 24 hours to begin the *Predictive Analysis* phase.

```
/*--------------------------------*- C++ -*----------------------------------*\
  =========                 |
  \\      /  F ield         | OpenFOAM: The Open Source CFD Toolbox
   \\    /   O peration     | Website:  https://openfoam.org
    \\  /    A nd           | Version:  8
     \\/     M anipulation  |
\*---------------------------------------------------------------------------*/
FoamFile
{
    version     2.0;
    format      binary;
    class       volScalarField;
    location    "0";
    object      k;
}
// * * * * * * * * * * * * * * * * * * * * * * * * * * * * * * * * * * * * //

dimensions      [0 2 -2 0 0 0 0];

internalField   uniform 3.201e-6;

boundaryField
{
    cylinder
    {
        type            fixedValue;                    (a)
        value           uniform 1e-30;
    }
    inlet
    {
        type            fixedValue;                    (b)
        value           uniform 3.201e-6;
    }
    outlet
    {
        type            zeroGradient;                  (c)
    }
    BaseAndTop
    {
        type            empty;                         (d)
    }
}


// ************************************************************************* //
```

Figure 6. Modified velocity field, *k*, file in the *0* directory. (a) At the cylinder a fixed value of 0 is assigned, as for a viscous wall. In contrast, (b) at the inlet (free stream) a value of 3.201×10^{-6} is assigned. (c) The outlet boundary is set to *zeroGradient*, as no flux returns to the flow domain. Finally, (d) the *BaseAndTop* boundary remains empty, as this is a two-dimensional simulation.

Example of Implementing Predictive Analysis

Once the simulation is complete, the resolved flow field is returned to the student for visualization in ParaView. Students are provided with solution files and postprocessing MATLAB scripts to extract surface and wake data, which serve as the predictive baseline to be validated in the wind tunnel.

The surface data provides pressure and skin friction distributions around the cylinder. Using these results, students are tasked with computing the pressure coefficient, C_p, for the converged solution:

$$C_p = \frac{p - p_\infty}{\frac{1}{2}\rho U_\infty^2} \tag{4}$$

Similarly, the shear stress distribution is analyzed to predict boundary layer behavior. Although the total drag for this configuration is primarily driven by pressure - rendering viscous drag nearly negligible - this metric is critical for identifying flow topology. Specifically, the first instance of a negative skin friction coefficient, $C_f < 0$, represents the onset of reversed flow. This provides the student with *a priori* location of the separation point, indicating exactly where experimental data collection must be intensified to accurately characterize the phenomenon.

The C_p distribution for the test case selected for this work is presented in Figure 7. The pressure profile is presented for the upper surface featuring a fully turbulent boundary layer in the trailing edge of the cylinder.

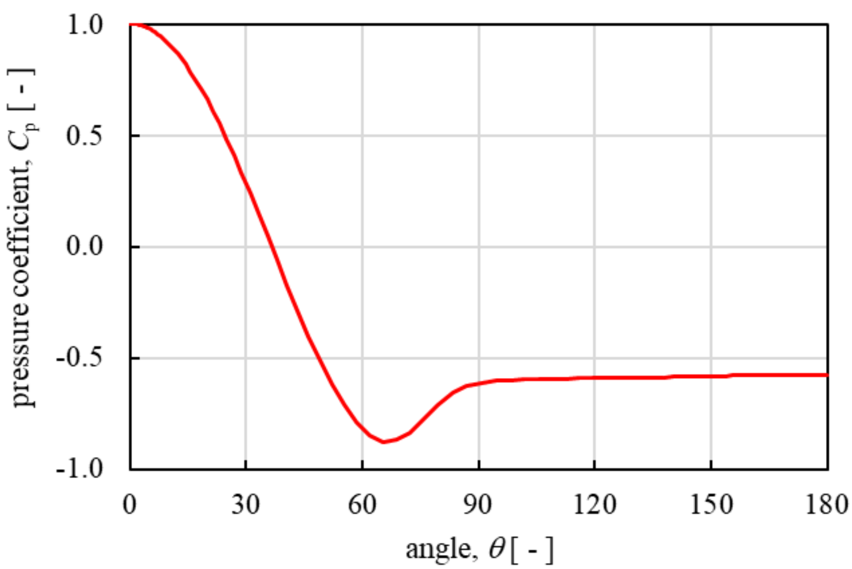

Figure 7. Computational Results. Pressure coefficient, C_p, distribution around the cylinder.

This is also confirmed by the C_f distribution presented in Figure 8, where a negative value is predicted suggesting the existence of reversed boundary layer characteristic of separated boundary layer flows.

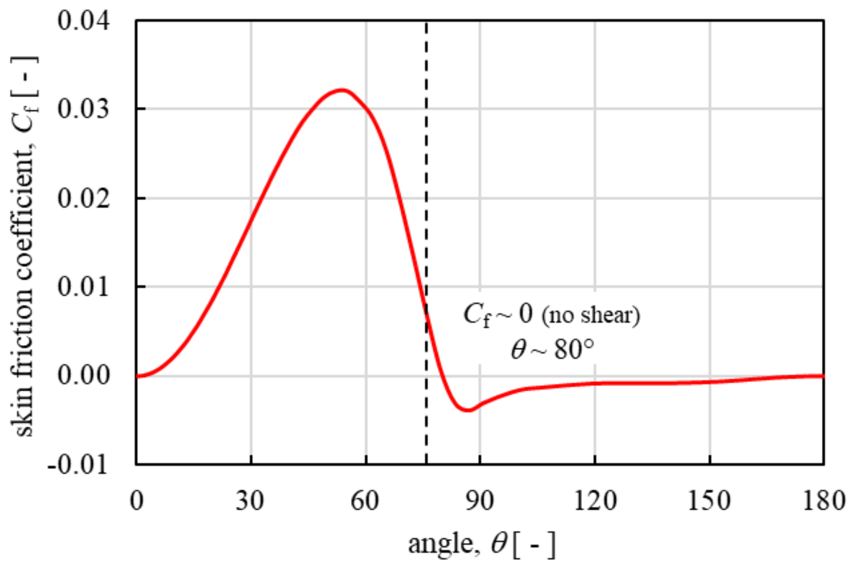

Figure 8. Computational Results. Pressure coefficient, C_f, distribution around the cylinder. The first negative value occurs at $\theta = 79.5°$, suggesting a separated boundary layer in that region.

Velocity and pressure contours provide a high-fidelity visualization of the flow as it separates from the surface and develops into a wake, as shown in Figures 9 and 10.

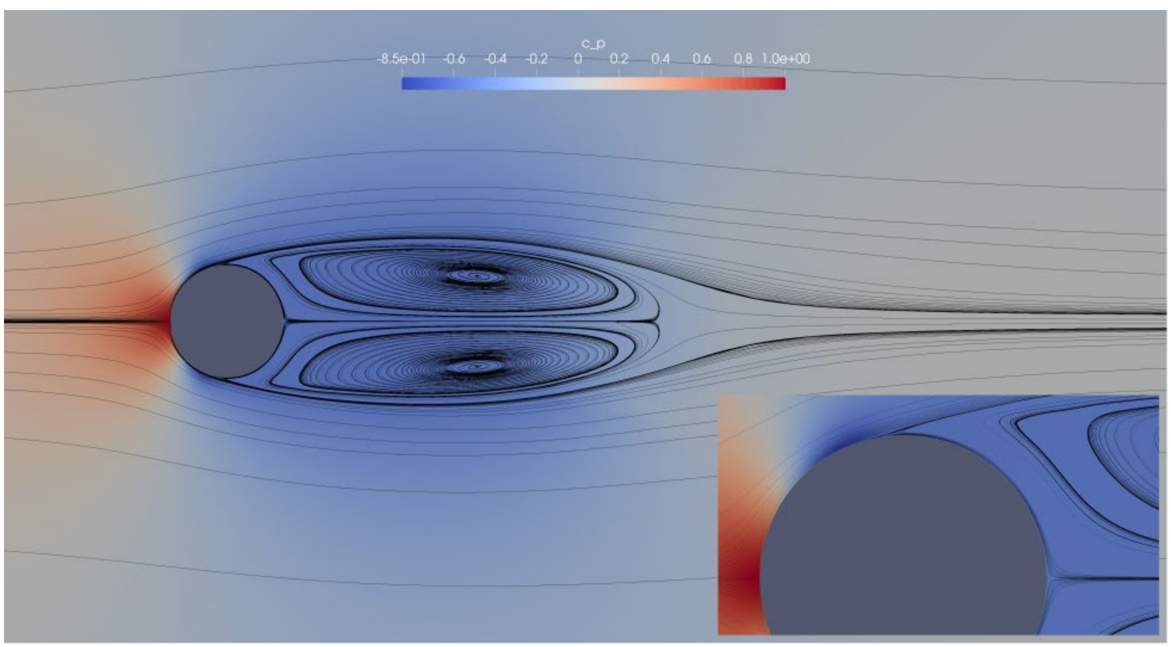

Figure 9. Pressure field contour. A detailed view of the pressure distribution near the upper half of the cylinder is provided. In the wake an apparent separated layer exists, with two vortices developing in the wake.

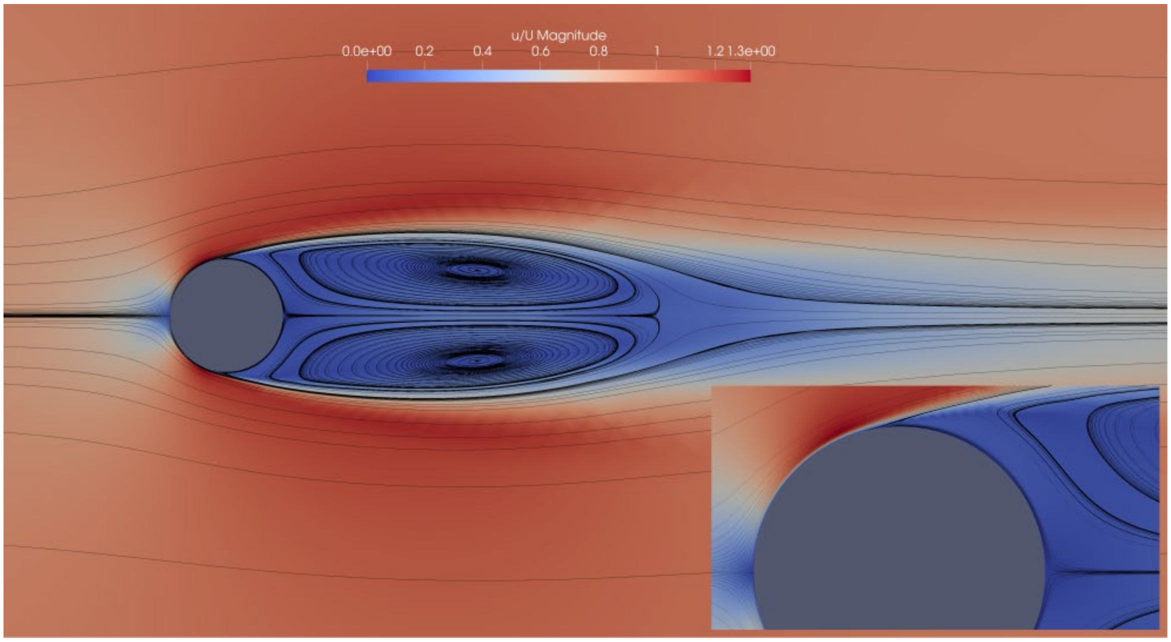

Figure 10. Velocity field contour. A detailed view of the streamlines is also provided. In the upper surface a separated layer exist, roughly downstream the 90 degrees mark.

To quantify the wake's behavior, students utilize virtual boundary probes placed at selected x/D distances downstream of the cylinder, as shown in Figure 11. These probes allow students to characterize the velocity deficit - the reduction in flow speed behind the body - and the spatial extent of the wake.

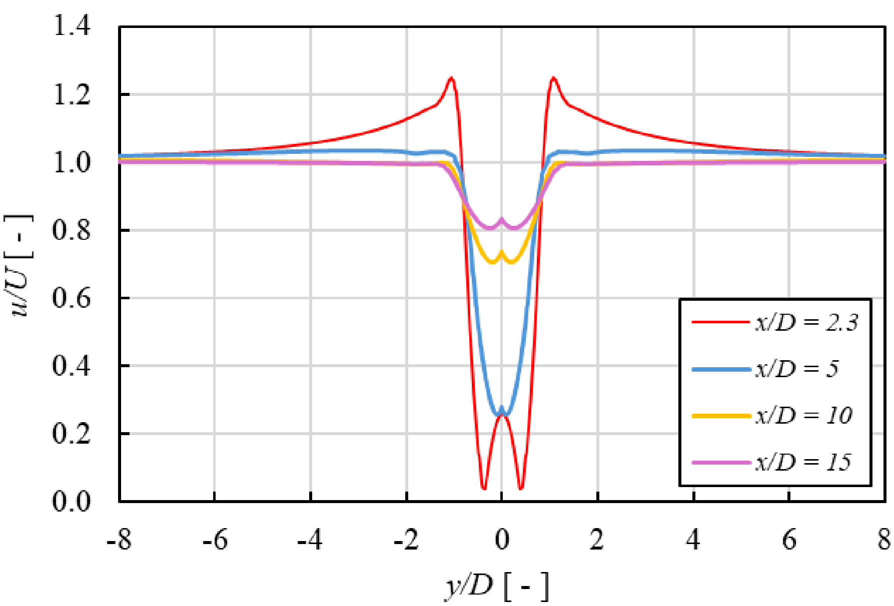

Figure 11. u/U (non-dimensional velocity) vs y/D (normalized vertical distance) for different x/D (dimensionless downstream) locations. For all different x/D values the width of the wake is in between $y/D = \pm 2$, suggesting a finer data acquisition in that region. Note that the cylinder centerline is at $x/D = 0$, so no upstream profiles are shown.

By analyzing these virtual probes before entering the laboratory, students can strategically plan the placement of physical instruments, i.e. Pitot tubes or anemometry sensors. This ensures that the experimental *Targeted Data Acquisition* captures the most critical gradients in the flow field, transforming the student from a procedural operator into a deliberate investigator.

Example of Implementing Experimental Design and Targeted Data Acquisition

With the computational results in hand, students proceed to a critical decision-making stage. In this phase, they must select a specific combination of instruments and define a spatial sampling strategy to validate their numerical results. This inquiry-driven stage should be guided by the instructor who can provide them with information as to available equipment for the experiment (without telling the students directly what to do – again the idea is to eliminate the student as simply following procedures). From the computational results, students should recognize that the CFD simulations can give them very detailed information about:

- The velocity field, broken into the simulated components, both close to and far from the cylinder (including velocity fluctuations through turbulent properties such as the eddy viscosity).
    - The velocity field can yield surface shear stress and the dimensionless form (the skin friction coefficient C_f).
- The pressure field both at the surface of the cylinder and away from the surface within the flow field.
- The drag force and drag coefficient (through knowledge of the pressure and velocity fields, i.e., the surface pressure and surface shear stress distributions).

A review of on-site available instrumentation, guided by the instructor, would lead students to understand just what kind of velocity and pressure information can be measured along with what spatial and temporal resolution. Furthermore, if a load cell is available, it is possible to directly measure the drag force in addition to the details that can yield drag through integration (refer to equation 2 earlier in the work).

<u>Instrumentation and Surface Pressure Strategy</u>

For this case, surface pressure measurements are limited to a single pressure tap on the cylinder surface. To obtain a full distribution, the cylinder must be rotated manually. Consequently, aside from selecting a pressure transducer with the appropriate range - as guided by the magnitude pressure distribution results - the primary task is to optimize the angular sampling rate.

Based on the CFD predictions, students identify regions where the flow is laminar and attached, such as the leading edge; in these areas, angular increments, θ, of 5-10° are sufficient. However, in the separation region predicted by the C_f distribution, students may decide to reduce the increments to a magnitude of 1°. Since drag in this bluff-body configuration is primarily pressure-driven, this high-resolution surface pressure distribution allows for a more accurate integration of the drag coefficient, C_D.

Wake Survey Optimization

A secondary method available in the laboratory for indirectly measuring drag is a wake survey. Computational results indicate that the region of interest for the wake - the velocity deficit zone - varies significantly as a function of the downstream distance, x/D.

Students use the CFD wake profiles to define the relevant vertical range, y/D, for their measurements at different x/D locations. By tailoring the survey grid to the predicted width and depth of the wake, experimental characterization becomes much more efficient. This refined survey ensures that the momentum deficit is captured fully, leading to a more reliable experimental calculation of the drag force compared to a generic, non-targeted survey.

Note that in a traditional laboratory exercise, the students are provided with instrumentation that has been determined to be sufficient (e.g., the range will work with the chosen flow field), and the dimensional constraints on something like a wake traverse is dictated to them. This is why, as we said before, the role of the student is more procedural rather than investigative. By using the CFD results to guide experiments, students take on a more investigative role with greater agency in the entire experiment process.

Example of Implementing Validation Experiments for CFD Study

The validation experiments that we have performed at Cal Poly for the purpose of this paper are based upon an existing traditional experiment [11], implemented for nearly 20 year in our engineering fluid mechanics laboratory class, that asks students to indirectly measure the drag on a cylinder in a cross flow arrangement using two techniques: (1) integrating surface pressure measurements (and neglecting skin friction drag due to the bluff body shape); (2) using a wake traverse method at one or more downstream locations and comparing the momentum flux at those locations to the idealized uniform momentum flux upstream of the cylinder. These are the learning objectives of the traditional lab. To accomplish the experiment, nothing more is needed than a pressure transducer, an instrumented cylinder with a single pressure tap (so that the tap can be rotated to effectively create a tap at any angle on the cylinder surface), and a Pitot-static tube mounted to an *xy* traverse.

Given that a discussion with students during the validation inquiry stage of the new lab module would involve introducing them to the available instrumentation (recall that we have mentioned that this part of the lab module would be site-specific), that discussion would inevitably lead students to a nearly identical set of validation experiments at our university. However, students should also recognize that since they can extract from their CFD simulations the degree of turbulence using the eddy viscosity, and the response rate of the pressure transduce used for measurements allows for the measurement of pressure fluctuations (i.e., the values on the display vary with time – about a steady average – in the turbulent regions of the flow), part of their validation experiments could incorporate probing which regions of the flow are highly turbulent, e.g., the wake. Thus, we present here the results of validation experiments that would logically follow from a guided discussion where students are first asked to think about what CFD results can be (or need to be) validated, then shown or otherwise given information about available equipment. These validation results are provided as an example to help guide an instructor interested in implementing this module at their home institution. More results are provided than would be expected out of a typical 2-3 hour block of lab time; however, the authors have chosen to show more to highlight the potential of the lab module.

Available Equipment and Instrumentation

The wind tunnel that was used for our site-specific example at Cal Poly is a commercially available ELD Model 406 that has a 2 ft. x 2 ft. test section cross section, a test section length of approximately 44 in. (with a practical length of 40 in. for the Pitot-static tube traverse), and a maximum test section velocity of up to approximately 110 mph (160 ft/s). Fan rotational speed, which directly controls test section velocity, is varied through the use of a variable frequency drive (VFD). This model of wind tunnel comes standard with a Pitot-static tube mounted on an *xy* traverse which is capable of measuring static, stagnation, and dynamic pressure at locations along the midplane of the test section (i.e., the Pitot-static tube is constrained to move in a plane and accesses the test section through a slot at the top of the wind tunnel – it is this slot that allows for the insertion of a tuft array as explained later on). A standard instrumentation box supplied with the tunnel provides a digital readout of Pitot-static tube *x* and *y* locations (in inches) in addition to a readout of differential pressure (when connected to the Pitot-static tube this provides dynamic pressure). The pressure transducer within the instrumentation box is a MKS Baratron© Series 200, with a resolution of 0.001 in.H_2O, and the system updates the digital readout every 0.5 seconds. This response rate means that fluctuations in pressure with timescales larger than 0.5 seconds can be observed and measured (unlike a liquid-filled manometer that would have a very long response time and thus would be insensitive to short timescale fluctuations); however, these fluctuations are in no way an accurate measure of the turbulent nature of the flow especially when one considers the influence of the measurements on tube length and tube compliance (i.e., the tubes connecting taps on instruments to the transducer). Even though we are not capable of measuring any turbulent characteristics with accuracy, out setup *does* allow for a pseudo-quantitative use of the fluctuations to determine which regions in the flow have larger or smaller fluctuations, or effectively no fluctuation at all. This allows us to conclude where regions of the flow are highly turbulent as compared to those with low or background levels of turbulence consistent with the free stream of the test section when no model is present. A collection of images showing the wind tunnel setup at Cal Poly is provided in Figure 12.

Although the wind tunnel also has a load cell for direct measurements of drag and lift forces on models, for the purposes of this module – which, again, emphasizes the importance of CFD validation as the rationale for experiments (rather than running experiments alone) – we have chosen to use as our model the cylinder provided by ELD. This is a 1.5-in. diameter smooth brass cylinder with a single static pressure tap. By rotating the cylinder along its access, the single tap can provide a measurement at any desired angle. Since this model is supported by the front and back walls of the wind tunnel with pins, and the ends of the cylinder are flush with the walls, the cylinder cannot be mounted to the load cell (hence the need for indirect measurements of drag through pressure and velocity). In addition, the wall-to-wall nature of the cylinder prevents flow of air around the ends and thus suggests that a 2D approximation to the flow field may be valid for analysis. In other words, it suggests that spanwise flow or spanwise variations may be negligible. Additionally, the frontal area of the cylinder accounts for only 6.3% of the test section, and so this low blockage ratio suggests that confinement effects, i.e., the influence of the walls of the wind tunnel, may be negligible; however, there are methods for correction that are beyond the scope of this project [12].

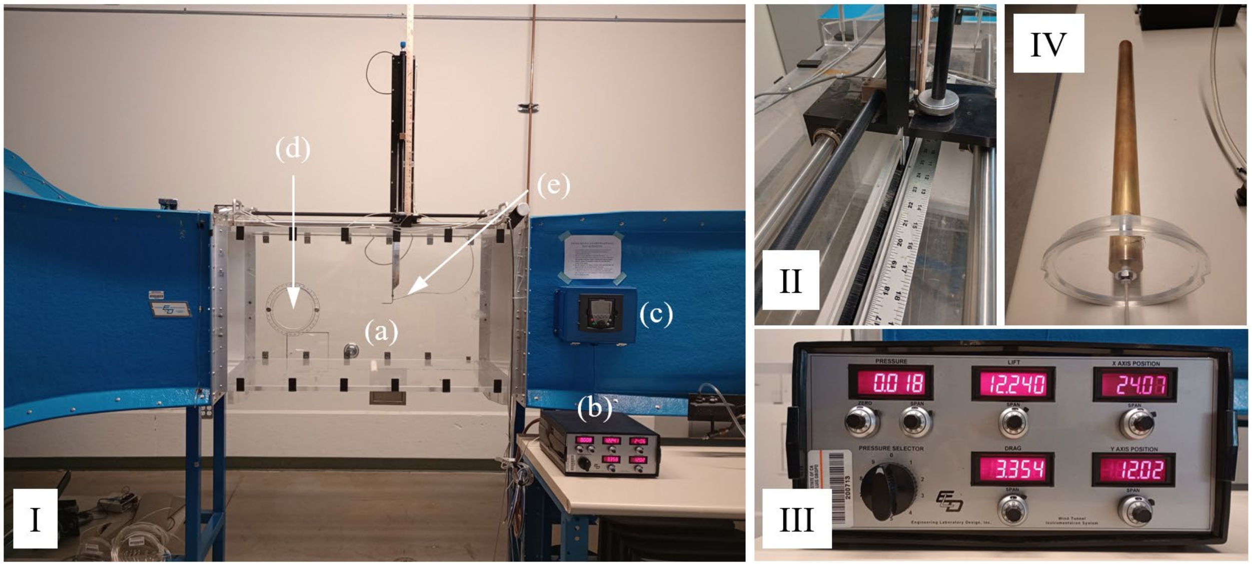

Figure 12. The fluid mechanics laboratory wind tunnel and instrumentation at Cal Poly. (I) A view of the ELD Model 406 wind tunnel showing the (a) test section, (b) instrumentation box, (c) VFD controller, (d) port to place cylinder model, and (e) Pitot-static tube on the x-y traverse. (II) View looking down onto the test section showing the slot in which the Pitot-static tube moves, which also provides access to the test section for a tuft probe. (III) Instrumentation box containing the differential pressure transducer and Pitot-static tube position readouts. (IV) The 1.5" brass cylinder with pressure tap supplied by ELD.

For our validation experiments, we have chosen to use a single test section velocity of 51 ft/s (20 Hz on our VFD controller) corresponding to a sub-critical Reynolds number of 40,000. The subcritical Reynolds number indicates that a laminar boundary layer will grow along the cylinder before it separates to form the wake. Our wind tunnel top speed and cylinder size limit our Reynolds numbers to be sub-critical unless the boundary layer is intentionally tripped on the cylinder (something that could become an additional choice in this lab module if students were tasked with performing a CFD study on a supercritical Reynolds number on the order of 200,000 or more). Additional variations of this lab module could include validating CFD studies that are performed at various test section velocities and Reynolds numbers, not to mention completely changing the model geometry to suit the equipment available on-site. The choice is ultimately dependent on the instructor, the time they and their students can invest in the lab exercise, and the creative aspects that they want to explore.

Given the wind tunnel and instrumentation available at Cal Poly just described, it is possible to measure details of velocity and pressure to validate the CFD model by comparing magnitudes, trends, and fluctuations in these quantities. We can further make sense of the CFD model by comparing not only these quantitative measurements but also through the use of qualitative flow visualization using tufts placed on the surface of the cylinder and on tuft arrays introduced in the test section. In what follows, we present the results of such experiments and compare CFD results to show what students might encounter as they attempt to validate their CFD models.

Velocity Field Measurements

Detailed measurements of velocity, along with measurements of pressure (which we will see in the next section), are two quantities that we can compare directly to the results of CFD simulations given that the wind tunnel setup at Cal Poly has a traversable Pitot-static tube but not a cylinder model that can be mounted directly to a load cell. We have chosen to make measurements traversing the test section from top-to-bottom (in the y-direction) at locations upstream of the cylinder, at the centerline of the cylinder (up to locations close to, but not at, the surface), and downstream of the cylinder. These would be traverses at different x-locations within the wind tunnel test section. At each measurement location, we collect 30 sequential readings of pressure from the display in order to determine an average value and standard deviation; the latter quantity being representative of turbulent fluctuations in the flow field at that point (but not an accurate measure of turbulent properties). Given the 2Hz frequency at which the pressure transducer display updates, the readings are extracted from a smart-phone movie that monitors the readout. By measuring velocity at the x-locations mentioned, we can determine the uniformity of the velocity profile upstream of the flow, the local acceleration of the air close to the cylinder, and the velocity defect in the wake. In addition, we can understand at what locations in the flow field we see measurable velocity fluctuations (through the calculated standard deviation about the average). Our CFD informs us that we ought to see significant fluctuations in the wake downstream of the cylinder, but outside of that region (both upstream and downstream), we expect to see insignificant fluctuation in the measured values.

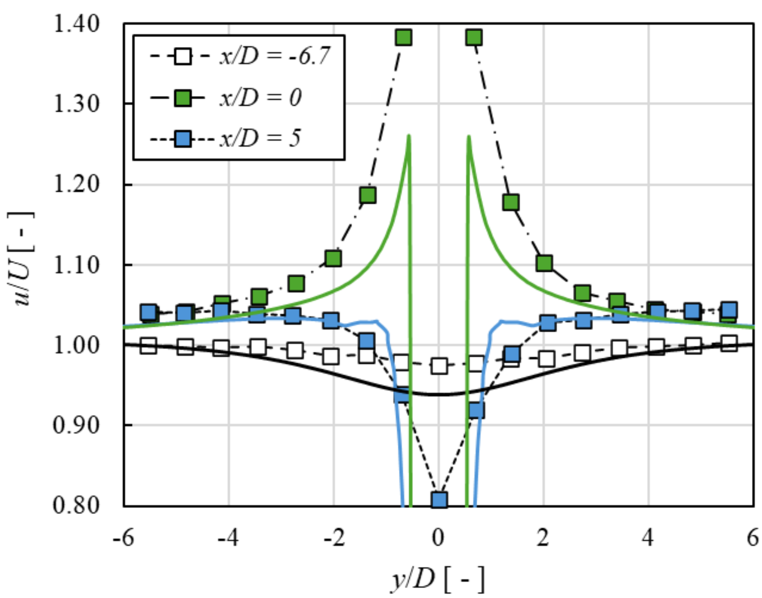

Figure 13. A plot of normalized velocity *u/U* (where *U* is measured far upstream of the cylinder at coordinate *x/D* = 0, *y/D* = 4) versus normalized vertical location *y/D*. Three measurement locations are shown (markers with dashed lines) and compared to CFD simulation results shown using solid lines.

The results of velocity measurements and velocity fluctuation calculations, along with the direct quantitative comparison to the CFD results, are presented in Figures 13 and 14. In Figure 13 we see a comparison between the magnitude of measured velocity and the results of CFD simulations.

The plot presents normalized quantities, i.e., u/U, which is typical. Each of the points on the plot represents an average of 30 sequential measurements at the same location. As expected, we see a nearly uniform velocity profile upstream of the cylinder; however, a slight defect (i.e., a reduction in velocity) is observed close to the cylinder centerline near y/D = 0. This suggests that the influence of the cylinder on the flow is felt far upstream of the cylinder (an interesting observation that is likely unexpected by students). At x/D = 0 (corresponding to a location aligned with the center of the cylinder), as the Pitot-static tube is moved closer to the cylinder either from the top or the bottom (in the y-direction), we observe an increase in the velocity u/U. This is expected as the air flowing around the cylinder must accelerate because of the change in the cross section. The experimental measurements terminate near y/D = ± 0.5 (the surface of the cylinder), but we cannot make a measurement at that precise location because of the thickness of the Pitot-static tube. Downstream of the cylinder, we can measure the velocity defect in the wake. At a distance of 5 diameters from the centerline, the extent of the wake is measured to be approximately y/D = ± 2.

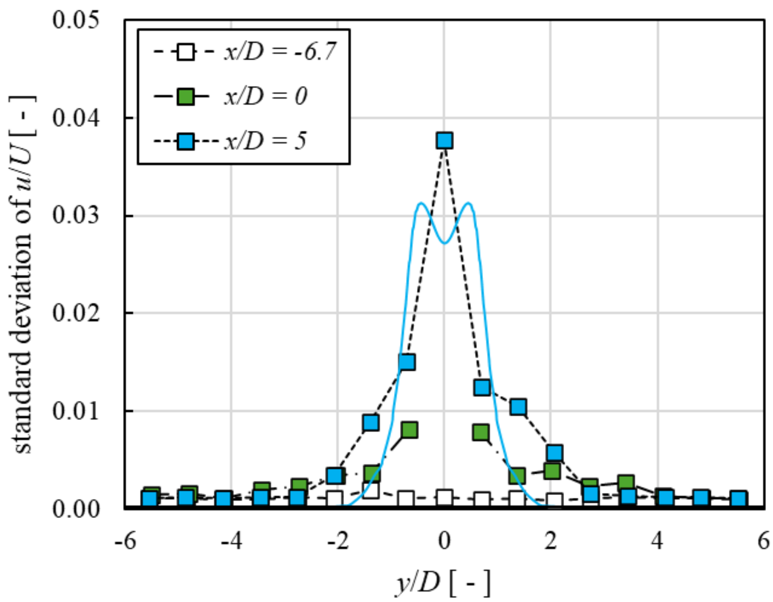

Figure 14. The standard deviation of normalized velocity measurements is plotted versus vertical position for the three *x/D* locations of Pitot-static tube traverses. Well upstream of the cylinder (*x/D* = -6.7) the variation in velocity measurements is negligible. At the cylinder centerline (*x/D* = 0) and more noticeably in the wake (*x/D* = 5), as expected, we see prominent fluctuations indicative of turbulence. CFD simulations only suggest noticeable eddy viscosity in the wake and are consistent in intensity with the results of experiments; however, the width of the region where this intensity is observed is narrower than that of the experiments. This is consistent with the wake size in Figure 11.

The CFD results are shown as solid lines in Figure 13. From the plot it is clear that while the CFD results mimic the qualitative behavior of the experimental results and are nearly identical in magnitude far from the cylinder (i.e., in y locations well away from the cylinder as u/U ~ 1), they fail to accurately predict the magnitude of velocity at these three locations. Interestingly, they predict smaller velocities along the cylinder centerline both upstream, at, and downstream (in the wake). The difference in the velocity defect in the wake is quite dramatic – so much so that it would distort the plot if shown completely. To quantify, the minimum value of the CFD results at

x/D = 5 is equal to $u/U \sim 0.3$. Even with these discrepancies, a student can understand the power of the CFD simulation in capturing many of the details of the flow field that are quite laborious to measure in the lab.

In addition to the measurements of velocity magnitude, we can use the multiple measurements (quantity of 30) at each location to extract a standard deviation. We use this as a proxy for turbulent intensity in the flow field, and we compare these measurements to the turbulent eddy viscosity that can be extracted from the CFD simulations. A direct comparison of measured and simulated quantities is shown in Figure 14.

In Figure 14, we see the practicality of using velocity fluctuations as a means of validating the CFD simulation predictions of turbulent intensity through the use of eddy viscosity. This useful and practicable even without tools specifically designed to accurately measure turbulent intensity, e.g., hot-wire anemometers or other high-speed velocity measurement/sampling instruments [13]. This should give students confidence in using this technique as a means with which to begin to validate the results of CFD experiments. However, it should be noted that in Figure 14 we still see the same difference in the extent of the wake that was seen in Figure 13, in addition to the CFD simulation not predicting noticeable eddy viscosity in the region near the cylinder at the centerline (which we see in our experiments but with a much lower magnitude than that in the wake).

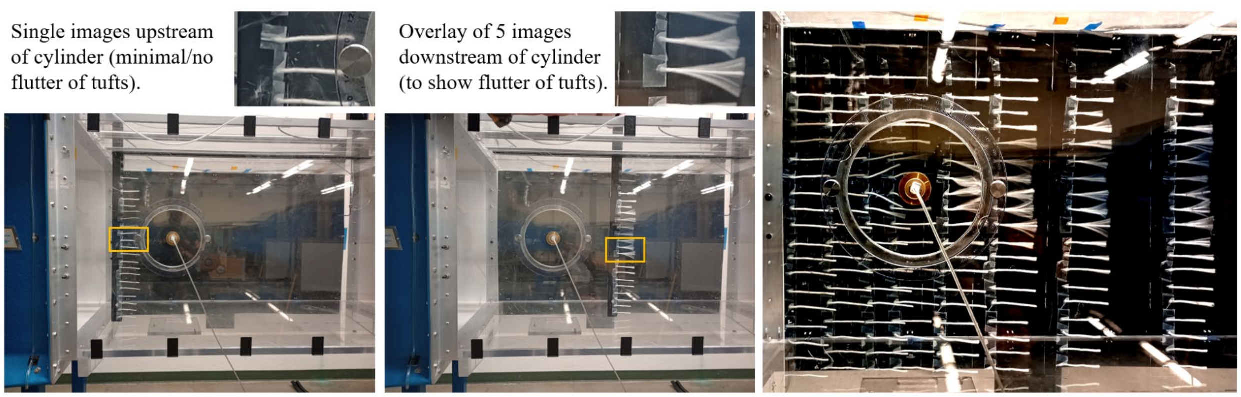

(a) (b) (c)

Figure 15. A panel of images showing the use of a tuft array stick to qualitatively show the flow field upstream and downstream of the cylinder. (a) When the tuft array stick is upstream of the cylinder, we observe a mostly uniform flow with only slight deflections of the tufts close to the cylinder centerline and increasing as we move closer to the cylinder in the *x*-direction. The inset of (a) indicates minimal flutter of the tufts in this region. (b) When the tuft array stick is downstream of the cylinder, we observe the wake through flutter and chaotic motion of the tufts. Within the wake, the superposition of multiple images leads to a blur of these tufts. Outside of the wake, the tufts are no longer blurred. (c) Using ImageJ, we can take multiple images, each with the tuft array stick at a unique *x/D* location, and "add" them together to create a complete image of the flow. For contrast we have added a black background to the test section, made the tuft array stick black, and have used white yarn tufts.

What remains for the velocity field is to explore it through the use of qualitative flow visualization at a level accessible to most undergraduate student aerodynamic experiments. By this we mean low-cost methods and those not requiring particular care and expertise (e.g., applications of liquid films or paints, particle image velocimetry, etc. [14]). For years now, the traditional experiment at Cal Poly has asked students to take a yard stick with incremented yarn tufts and place it into the test section using the slot in the top of the wind tunnel (cf. Figure 15). While this is a starting point to qualitatively observe the flow, students have never been asked to do anything more than notice the difference in what they see if they move the yard stick from upstream of the cylinder to downstream of the cylinder. We propose, and are working to implement, a technique, whereby students can more carefully locate one of these tuft array sticks, take images, and then superimpose the images so that they can create a full picture of the tufts covering the entire flow field of interest. In this way, the direction of the tufts is an indicator of the direction of velocity vectors, and the blurriness of the tufts (achieved by superimposing multiple images taken with the stick at the same location) is representative of regions of the flow where there is turbulence – for example this is anticipated in the wake but not outside of the wake. Despite the simplicity, the use of tufts for flow visualization has many advantages [15]. This is a low-cost flow visualization method that requires simple tools provided by the lab instructor (or constructed by the students), a tri-pod mounted cell phone for images, and open-source image processing software like ImageJ for superposition of photos [16].

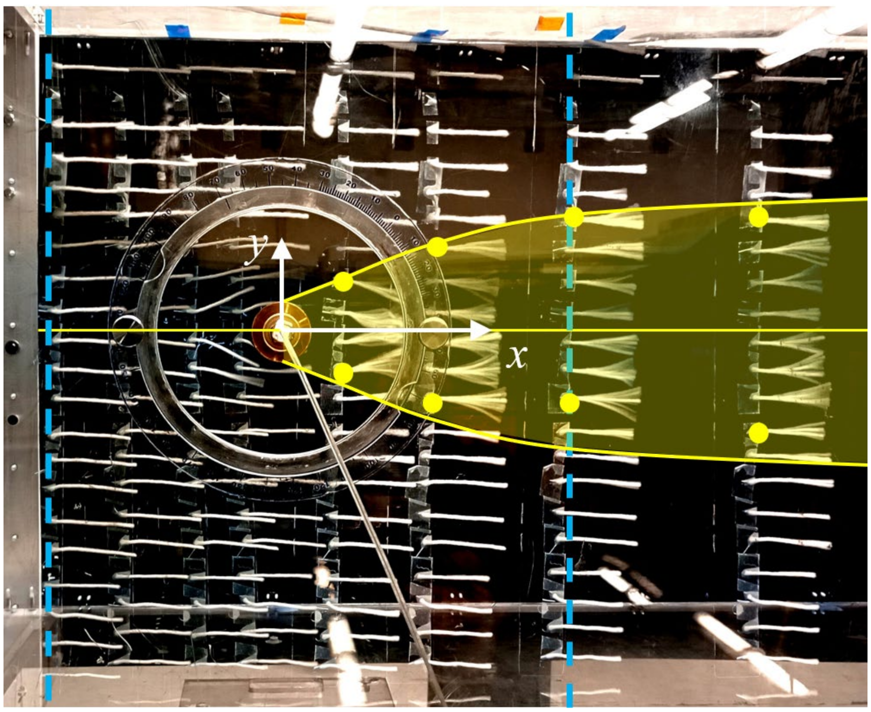

Figure 16. A superposition of tuft array stick images is shown. Manually looking for where tuft flutter occurs allows us to identify the approximate edge of the wake (yellow dots). A crude fit of a line through the dots and then mirroring this from top to bottom helps show the extent of the wake (which is given a light-yellow color). In this way, the size of the wake spans approximately ± 2*D* at the *x/D* = 5 location (the dashed blue line downstream of the cylinder).

Figure 15 highlights this flow visualization technique that we have employed. Although we cannot use this flow visualization technique to make any quantitative measurements of velocity magnitude, we can quantify the size, i.e., vertical extent, of the wake downstream of the cylinder by observing where tuft flutter becomes obvious. By looking for this flutter, or blurriness, at each location along the tuft stick, we can place a marker where we think the edge of the wake is. Connecting these markers allows us to "see" the evolution of the wake downstream of the cylinder which we can relate back to the quantitative velocity measurements in Figure 13. What we describe here of determining the wake extent by the flutter/blurriness is shown in Figure 16. Additionally, an overlay of what we believe is the wake from Figure 16 onto an image of the eddy viscosity plot from the CFD results provides an excellent visual with which to understand validating the CFD. This visual construction is shown in Figure 17. In both figures, the vertical light blue lines represent locations of x/D = -6.7 (upstream of the cylinder) and x/D = 5 (downstream of the cylinder). What we see in Figure 17 is consistent with the quantified velocity measurements (both velocity magnitude and standard deviations). Namely, the extent of the wake in the y-direction is larger in the experiment than is predicted by the CFD simulation.

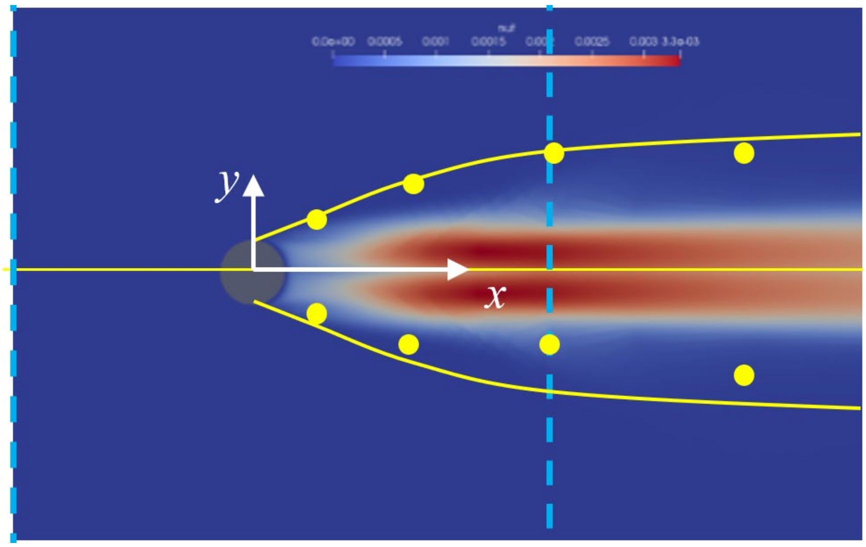

Figure 17. Transferring the manually determined edge of the wake from Figure 16 (yellow dots and yellow lines) onto a CFD simulation of eddy viscosity shows that the extent of the simulated wake is smaller than that of the simulation – a result consistent with other quantitative measurements of velocity.

<u>Pressure Measurements</u>

Static pressure in the flow field can be measured by traversing the Pitot-static tube with the total pressure disconnected and directly measuring the static pressure on the surface of the cylinder using the tap on the cylinder (which can be rotated to measure the static pressure at any angle). We chose here to report measurements of static pressure on the surface of the cylinder which is consistent with one of the objectives of the traditional experiment that our lab module is intended to replace at Cal Poly.

As with the measurements and comparisons of velocity, we choose a dimensionless representation of pressure in our reporting. The choice is to use the pressure coefficient, C_p, which is defined as the static gage pressure divided by the free stream dynamic pressure (measured upstream and above the cylinder at a location x/D = 0 and y/D = 4). And also like velocity measurements, we can take multiple measurements of pressure at any angular location so as to calculate an average value and a standard deviation of the measurements. The fluctuation in the surface pressure measurements (quantified through the standard deviation) sheds light on where the boundary layer separates from the surface of the cylinder. It is this separated boundary layer that gives rise to the turbulent wake. Thus, we anticipate that separation on the surface corresponds to where pressure fluctuations dramatically increase.

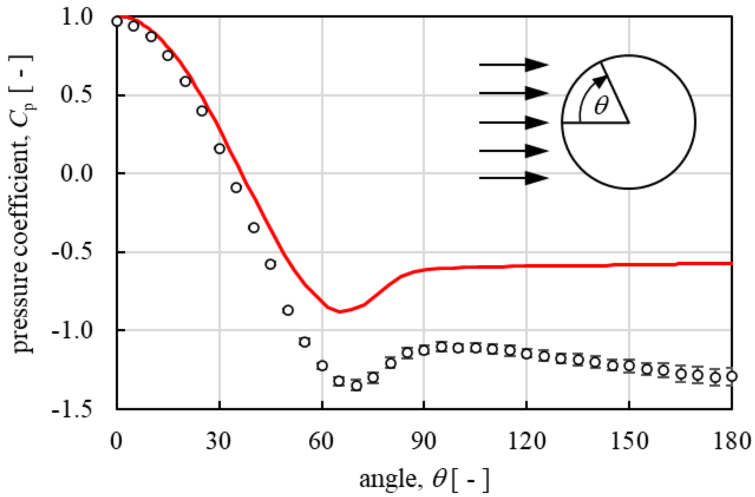

Figure 18. A comparison of pressure coefficient values between experimental measurements (open markers) and the CFD simulation (solid red line). The meaning of the angle along the cylinder is shown in the inset diagram with 0° being the leading edge of the cylinder.

Figure 18 shows the comparison between measured values of the pressure coefficient to those predicted from the CFD simulation. There is excellent agreement near the leading edge of the cylinder, but as the angle increases, so does the difference in the magnitude of the pressure coefficient (albeit with similar trends). Where the values of C_p become nearly constant with increasing angle (beginning around 80° – 90°), this is where boundary layer separation is predicted as the pressure in the wake is known to be both approximately constant along the surface of the cylinder and similar in magnitude to that at the point of separation. So even though the C_p values are different between the measurements and the CFD simulation, nearly the same location of boundary layer separation is predicted. Given that we have seen differences in the size of the wake between the CFD simulation and the experiment, we anticipate that the difference in C_p values in the wake region is related to this.

For the sub-critical Reynolds number for this experiment and simulation, a laminar boundary layer forms on the cylinder surface before it separates to form a turbulent wake. As the wake is a region of turbulence and mixing, we expect that pressure fluctuations measured at the surface will be larger in the region surrounded by the wake as compared to the pressure fluctuations (if at all) measured nearer to the leading edge. To show this, we can compare the fluctuations in the measured pressure coefficient (quantified by the standard deviation of 50 measurements) to the fluctuations of the pressure coefficients obtained from the CFD simulation. For the latter, the fluctuations represent the small variations that exist in consecutive iterations after the convergence criteria have been met. This allows us to account for the fluctuations arising from the steady-state vortices generated in the wake immediately downstream of the cylinder. In contrast, the experimental data actually accounts for pressure fluctuations due to the oscillating nature of the configuration under study. Because these two things are different in nature but related to the turbulence of the flow, we don't expect the magnitudes of the two values to be the same, but we do expect a similarity in the trends. This is why the experimental data and the CFD simulation results in Figure 19 are plotted on axes with two different ranges (experimental values on the primary vertical axis and CFD simulation results on the secondary vertical axis). A crude comparison of the two sets suggests a similarity in boundary layer separation location consistent with the pressure coefficient measurements.

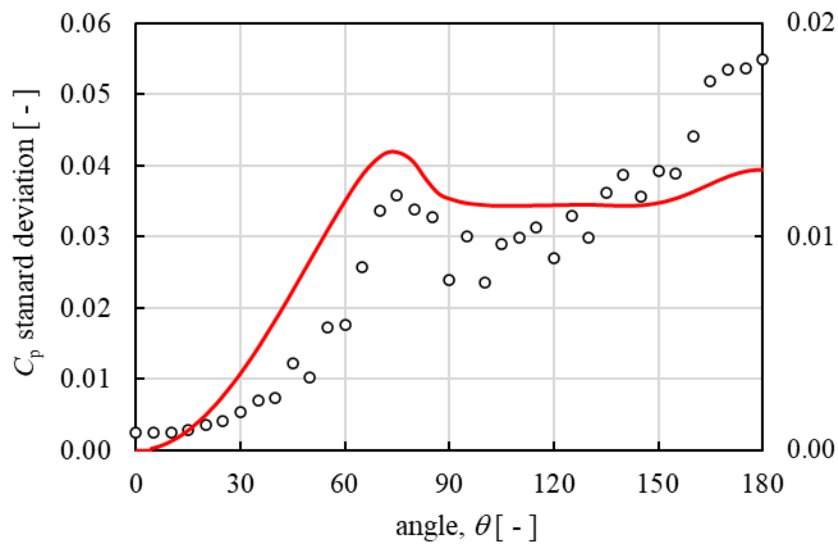

Figure 19. Pressure coefficient fluctuation comparison on the surface of the cylinder. The experimental pressure coefficient fluctuation (open symbols) is nothing more than the standard deviation of the 50 measurements taken at each angle. The CFD simulation fluctuation arises from the steady state vortices in the wake region at 50 consecutive iterations and is plotted using the secondary axis as the magnitudes of the two quantitative measures are not expected to be similar. More importantly, the trends in the two quantities are surprisingly similar and helps to validate that the CFD simulation is predicting a correct location for boundary layer separation.

Finally, a low-cost but effective flow visual can be had by attaching small thread tufts to the surface of the cylinder to visually confirm the location of boundary layer separation. As with the tuft array stick in the wake, the regions of turbulence – which correspond to the wake formed by the boundary layer separation - yield tufts that appear blurred in images. Rather than placing tufts at locations all over the surface of the cylinder, we have chosen to locate them in a patch near the end of the cylinder and close to the wall of the tunnel (for ease of taking photos). Since we can rotate the cylinder, we can rotate this patch of tufts. When the tufts are far from the separation point, the tufts lie mostly flat along the cylinder. We can see this behavior in the tufts pointed to by blue triangles in Figure 20(A). The tufts that are completely beyond the point of separation – in contact with the wake – are blurry and flutter dramatically. This is shown by the tufts pointed to by the red triangles in Figure 20(A) and (B) along with all the tufts in Figure 20(C) and (D). When the free ends of the tufts just approach the point of separation, they just begin to flutter. While this is currently difficult to see in these images, we can begin to make out this behavior as indicated by the yellow arrow in Figure 20(B). From this crude flow visualization, we can estimate boundary layer separation to occur at ~85°.

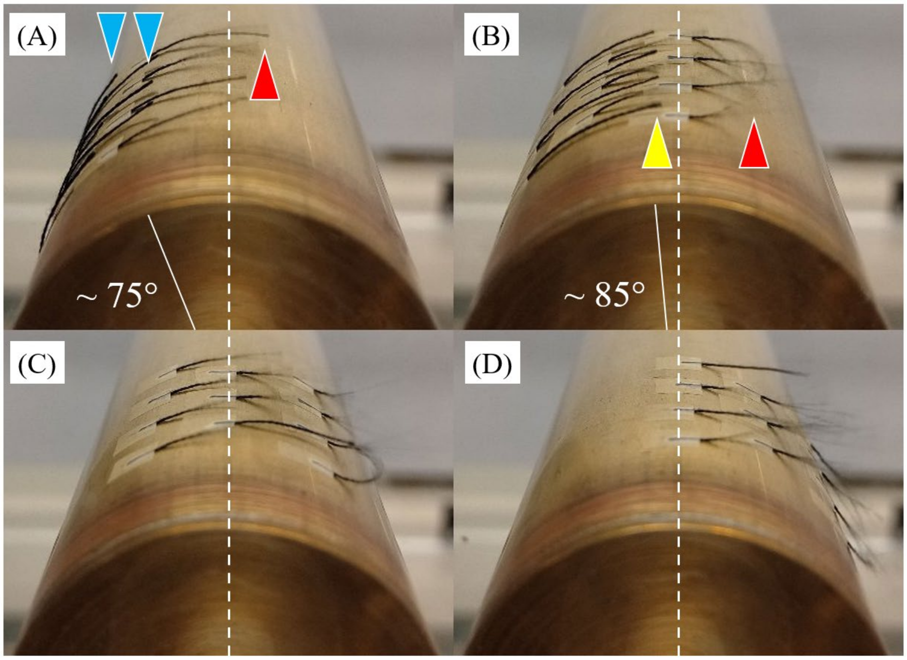

Figure 20. Flow visualization of boundary layer separation using thread tufts taped to the surface of the cylinder and rotated to effectively create tufts at different angular locations. Flow of air is from left-to-right. We anticipate boundary layer separation to occur at approximately 85° from this visual.

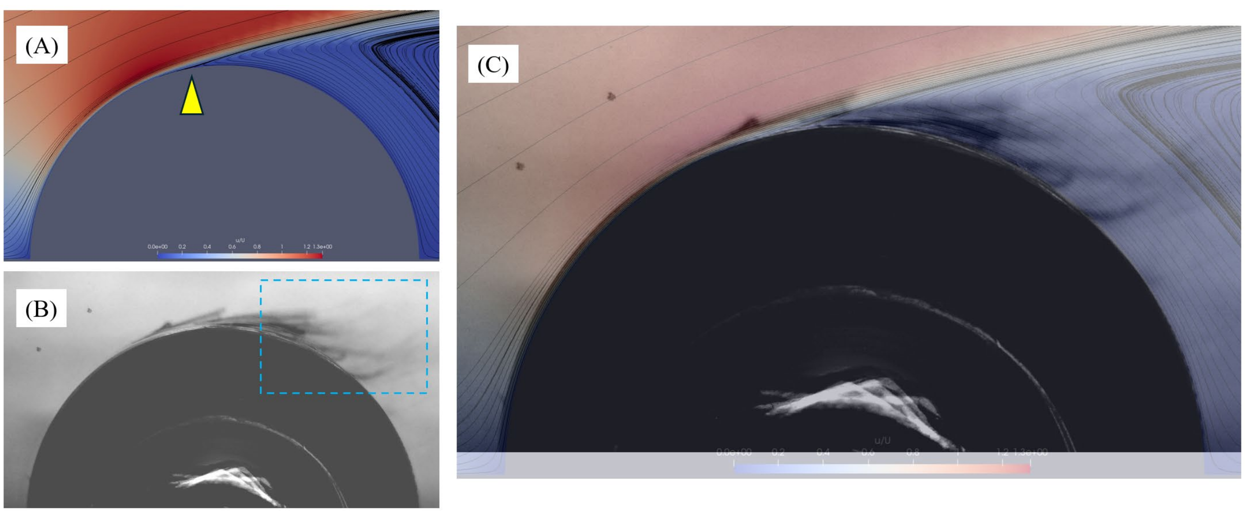

Figure 21. Direct visual comparison of CFD simulation results and cylinder surface tufts. (A) A flow field plot from the CFD simulation showing regions of high (red) and low (blue) velocity near the surface of the cylinder. Flow reversal and boundary layer separation is indicated using the yellow triangle – note that it is just forward of 90°. (B) A superposition of four tuft images provides a collection of un-blurred and blurred tufts along the cylinder surface. The tufts are most blurred in the region indicated by the blue dashed box. (C) Overlaying the CFD simulation on the cylinder tuft image shows an excellent qualitative agreement.

As with the superposition of yarn tuft images onto flow field images as in Figure 16, we can do the same here with the tufts on the surface of the cylinder. In Figure 21(A) we can see the results of the CFD simulation in which velocity magnitude (through color) and streamlines (black lines) are shown in a close-up image near the cylinder surface and viewed along the axis of the cylinder. The low velocity blue region downstream of the point indicated by the yellow arrow is the wake. Figure 21(B) is the superposition of four images of cylinder tufts, each with the tufts rotated to a different location along the surface and taken from a frame of reference directly in line with the axis of the cylinder (unlike the images of Figure 20 where the camera is elevated and looking down on the cylinder). The color of the image has been adjusted to better highlight the movement of the tufts. The blue box shows where they are the most blurry because of the turbulent motion. When we scale the images of Figure 21(A) and 21(B) and overlay them to form the composite image/plot in Figure 21(C), we see excellent qualitative agreement between the CFD predicted region of the wake and that observed in experiments. This helps provides yet another example of a type of validation scheme for the CFD simulation that undergraduate engineering students can implement and appreciate.

Investigating Discrepancies – Validation Inquiry

After comparing the results between experiments and CFD simulations, it is clear that there are quantitative discrepancies which offer students the opportunity to reflect on whether the experiments are flawed or whether the CFD simulation – which is approximate – does not sufficiently capture the relevant physics of the real flow field. While this opportunity exists in a traditional experiment (e.g., “Why does my calculated drag coefficient not match what I expect from the textbook?”), with the computational-experimental methodology, a richer investigation can be accomplished because of the detailed nature of the CFD results.

Barring all experimental measurement and calculation errors, the laboratory instructor should guide the students back to assumptions and approximations made when setting up the CFD simulation. The two most obvious potential sources of discrepancy are:

1. The flow around the cylinder is modeled such that the cylinder is in an infinite (i.e., unbounded) fluid. As such, there are no “walls” or confinement effects – or at least they are not as prominent – in the CFD simulation as compared to the experiment.

2. The simulation treats the flow as 2D, and this was chosen since the cylinder in the experiment is long in comparison to its diameter and it spans the entire test section preventing flow around the ends.

These two potential sources of the discrepancy between experimental results and simulation results can stimulate questions about whether they can actually account for the discrepancy. For example, would confinement of the flow cause velocities and pressures in certain regions to be lower or higher than expected? Would 3D flow effects – possible in the experiment despite the model shape – cause velocities and pressures in certain regions to be lower or higher than expected?

If limited time in the laboratory course dedicated to this one experiment prevents students from running a more complete simulation (e.g., accounting for the wind tunnel walls and/or accounting for 3D flow), qualitative answers to these questions are possible with physical explanations, e.g., confinement, or a reduction in flow passage area, will cause velocities higher than expected as dictated by conservation of mass. But quantitative answers are possible with more detailed CFD simulations that students can be guided through.

Assessment Plan

Although this paper has outlined a new methodology with which to transform a traditional undergraduate fluid mechanics laboratory experiment and has provided an example of the CFD and experimental results that can be obtained and compared, we have yet to implement the complete exercise in a teaching laboratory with students. The intent is to accomplish this during the 2026-2027 academic year when we can offer both the original format of the lab alongside the new framework. When we have the opportunity to do this, we plan to assess the effectiveness of this new approach.

To evaluate the effectiveness of the blended experimental-computational methodology, a comprehensive assessment framework is proposed to measure student attainment of outcomes aligned with ABET Criterion 3 [1]. The plan centers on capturing the development of "engineering judgment" by measuring the transition from procedural task execution to informed experimental design. This multi-faceted approach utilizes direct assessment through the evaluation of student-developed artifacts—specifically, a "Predictive Analysis Report" where students must justify their experimental parameters (such as sensor placement and sampling rates) based on their preliminary CFD findings. These artifacts will be assessed using standardized rubric to determine the student's ability to interpret numerical uncertainty and apply it to physical measurement strategy. Complementing this, indirect assessment will be conducted via pre- and post-module surveys designed to gauge shifts in student confidence, engagement, and their perception of the investigative nature of the lab. By comparing performance metrics between laboratories utilizing this integrated workflow and those following traditional formats, the authors aim to provide a data-driven validation of the methodology's impact on student agency. This framework is designed to facilitate a cycle of continuous improvement, ensuring that the integration of computational tools directly enhances the critical learning objectives of the fluid mechanics curriculum.

Conclusions and Future Work

In this paper we have presented a new methodology, a blended computational-experimental methodology, for operating a laboratory experiment that provides students an introduction to a modern computational tool (e.g., CFD), rethinks the experiment as a validation of the computational method, requires students to use the results of the CFD to inform and guide the experiment (e.g., regions of the flow to investigate, quantify limits to measurements regions, etc.), and then directly compare experimental results to computational solutions and inquire about the discrepancies if they exist. This methodology gives students a better understanding of the role of experiments in modern engineering problem solving and gives them far more agency in the experiment as compared to a traditional approach wherein they tend to merely follow a procedure in the lab environment. The example that we have chosen involves flow over a cylinder using a standard wind tunnel to show that currently existing experiments in undergraduate engineering fluid mechanics labs are amenable to this new framework. By shifting the experiment to a CFD validation, incorporating more flow visualization and imaging, and making direct comparisons between these quantitative and qualitative results with the CFD solutions, the laboratory experience can be much more rewarding and valuable for students all the while building on the established objectives and outcomes.

The future work for this project involves implementing the new methodology and analyzing the education effectiveness and impact as indicated in the assessment plan. The faculty authors look forward to completing this in the upcoming academic year with the many colleagues that are assigned to teach the laboratory. Future work also includes some minor additions to the experimental setup at our site. It should be noted that implementing experiment modifications using student assistants is another way to give students hands-on experiences and greater agency in the lab. For our project, we are involving students in both the development of the CFD tools that are critical to the new methodology and in the wind tunnel instrument modifications. Two examples include: (i) having students find the optimal lighting conditions and external wind tunnel covering materials for high-quality tuft photographs (challenging because of the reflective surfaces of the wind tunnel test section), and (ii) the design and fabrication of an updated moveable tuft array.

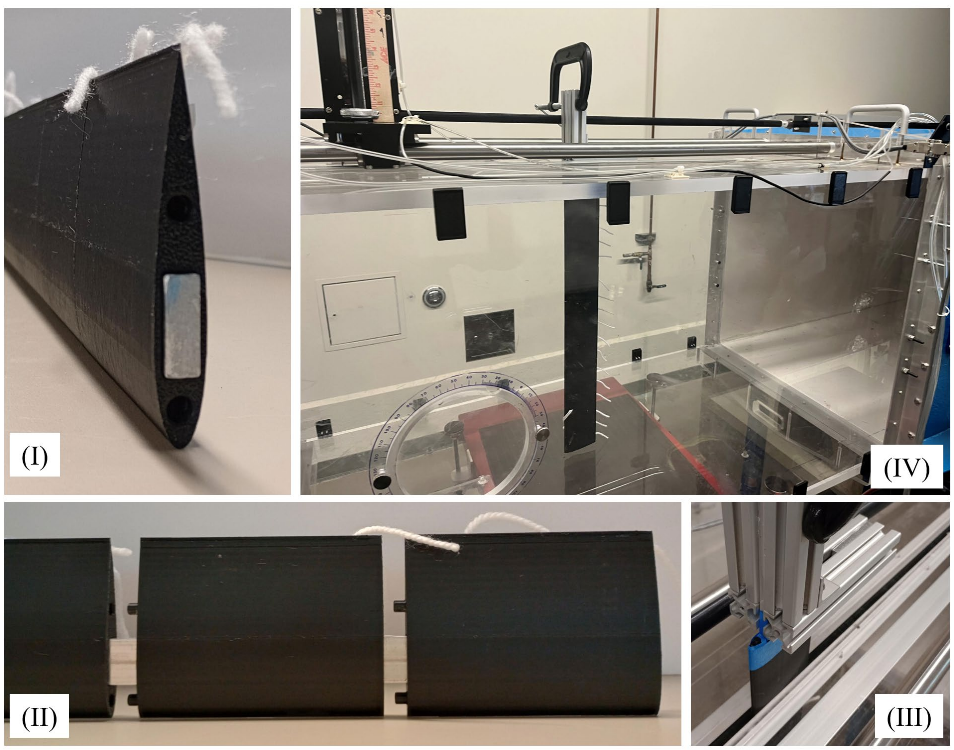

Figure 22. Student-designed tuft array for use with the wind tunnel experiment. (I) The cross section of the tuft "stick" will have a symmetric airfoil cross section to reduce the influence of the stick shape on the tuft motion. (II) The airfoil sections are 3D printed in pieces and placed along a solid metal spine. (III) The array can be placed within the same slot that allows for Pitot-static tube motion (with the maximum thickness of the airfoil shape matching the slot width). (IV) View of the new tuft array in the wind tunnel test section.

Acknowledgements

All authors would like to acknowledge the California Polytechnic State University San Luis Obispo for the use of wind tunnel time in the ME Fluid Mechanics Laboratory during the 2025-2026 Academic Year. Likewise, the authors would like to acknowledge Mr. Brandon Escobar and Mr. Jamie Feinstein, two senior undergraduate mechanical engineering students, for his valuable contributions to the experimental setup and implementation of the methodology presented in this paper. Author A. Cajal acknowledges the ME Department at the California Polytechnic State University for the release time for teaching afforded for scholarship as part of his Teaching Post-Doc Position. Finally, Cajal would like to thank the Aerodynamic Design and Research Laboratory at the University of Southern California, for facilitating the software to generate the grids for this study.

References

[1] Hailey, C. E., & Spall, R. E. (2000). *An Introduction of CFD into the Undergraduate Engineering Program*. ASEE Annual Conference Proceedings, Session 1566.

[2] Manzo, M. (2024). *Introducing CFD Concepts in an Applied Fluid Mechanics Course*. Proceedings of the 2024 Conference for Industry and Education Collaboration (CIEC), ETD 515.

[3] R. Medina, A. Motamedi, M. Okcay, B. U. Oztekin, and G. B. Menezes, "On the Implementation of Open Source CFD System to Flow Visualization in Fluid Mechanics," in *Proceedings of the 2012 ASEE Annual Conference & Exposition*, AC 2012-5482, 2012.

[4] N. Kim, "Importance of CFD in undergraduate-level fluid dynamics course," in *Proceedings of the 2024 ASEE Annual Conference & Exposition*, 2024.

[5] W. Mokhtar, "Project-Based Learning (PBL) An Effective Tool to Teach an Undergraduate CFD Course," in *Proceedings of the 2011 ASEE Annual Conference & Exposition*, AC 2011-973, 2011.

[6] K. Aung, "Design and Implementation of An Undergraduate Computational Fluid Dynamics (CFD) Course," in *Proceedings of the 2003 ASEE Annual Conference & Exposition*, 2003.

[7] M. N. Sarimurat, "Integrating Theory and Practice: A CFD Education Approach," in *Proceedings of the 2024 ASEE Annual Conference & Exposition*, 2024.

[8] General Criteria for Baccalaureate Level Programs – Criteria 3. Student Outcomes
Retrieved from: https://www.abet.org/accreditation/accreditation-criteria/criteria-for-accrediting-engineering-programs-2026-2027/

[9] J. W. Mitchell, "External Incompressible Viscous Flow: Drag," in *Fox and McDonald's Introduction to Fluid Mechanics*, 10th ed. New York, NY, USA: Wiley, 2020, ch. 9

[10] Menter, F. R., "Two-equation eddy-viscosity turbulence models for engineering applications", AIAA Journal, 32(8), 1598–1605. https://doi.org/10.2514/3.12149

[11] (Laboratory Manual – California Polytechnic State University)

[12] A. Pope, "Wind-Tunnel-Boundary Corrections," in *Wind-Tunnel Testing*, 2nd ed. New York, NY, USA: John Wiley & Sons, 1954, ch. 6.

[13] C. Tropea, A. L. Yarin, and J. F. Foss, "Velocity, Vorticity, and Mach Number: Thermal Anemometry," in *Springer Handbook of Experimental Fluid Mechanics*, 1st ed. Berlin, Germany: Springer Berlin, 2007, ch.5

[14] A.J. Smits and T.T. Lim, *Flow Visualization: Techniques and Examples*, 2nd ed. World Scientific Publishing Company, 2012.

[15] W-J. Yang, "Tufts," in *Handbook of Flow Visualization*, 2nd ed. Taylor & Francis, 2001, ch. 9.

[16] ImageJ Software, Retrieved from: https://imagej.net/ij/